

Subpicosecond Observation of Thermalization and Relaxation of Photoexcited Carriers in InP Based Films

J. Michael Klopf^{a)}, Andrew N. Smith^{b)}, John L. Hostetler^{c)}, Pamela M. Norris^{d)}

^{a)} Dept. of Engineering Physics, University of Virginia, Charlottesville, VA

^{b)} Dept. of Mechanical Engineering, U. S. Naval Academy, Annapolis, MD

^{c)} Princeton Lightwave, Inc., Cranberry, NJ

^{d)} Dept. of Mechanical and Aerospace Engineering, University of Virginia, Charlottesville, VA

ABSTRACT

Advancements in microfabrication techniques and thin film growth have led to complex integrated photonic devices. The performance of these devices relies upon precise control of the band gap and absorption mechanisms in the thin film structures, as well as a fundamental understanding of the photoexcited carrier thermalization and relaxation processes. Using a pump-probe technique, it is possible to monitor the transient thermalization and relaxation of hot electrons and holes on a sub-picosecond timescale. This method relies upon the generation of hot carriers by the absorption of an intense ultrashort laser pulse (~135 fs). Transient changes in reflectance due to the pump pulse excitation are monitored using a weaker probe pulse. Control of the relative time delay between the pump and probe pulses allows for temporal measurements with resolution limited only by the pulse width. The transient change in reflectance is the result of the transient change in the electron and hole distributions. Observation of the reflectance response of InP films on a sub-picosecond timescale allows for detailed examination of thermalization and relaxation processes of the excited carriers. Longer timescales (> 100 ps) are useful for correlating the transient reflectance response to slower processes such as thermal conduction and recombination. A description of this technique and results for several InP based films are presented.

INTRODUCTION

The continuing development of solid state photonic devices based upon various III-V semiconductors has created numerous advances in the technologies associated with communications, data storage, laser machining and cutting, and biomedical applications, as well as in many fields of basic science research. These small devices have very low power requirements, and can be integrated directly with power and control electronics, resulting in optoelectronics that are more efficient than multi-component systems. The production of passive elements such as wave-guides or active elements, such as amplifiers and switches, combine to expand the capabilities greatly. These devices rely upon layers of band gap engineered materials with critical dimensions on the order of nanometers.² The resulting interfaces create localized changes in the band structure which can affect absorption and recombination processes.^{3,4} Continued developments require ongoing research into the carrier dynamics in bulk materials as well as nanostructures.

Photonic semiconductor materials generally exhibit a direct band gap electronic structure. The direct alignment of the conduction band minimum and valence band maximum makes radiative recombination of electrons and holes very likely. This gives rise to many of the photonic properties of interest. The generation of excess conduction electrons is possible through the absorption of photons with energy, E_g , greater than the band gap, E_g . Since recombination of these electrons occurs primarily near the conduction band minimum, energy in excess of the band gap, $E_D = E_g - E_g$, must be transferred to the crystal through relaxation processes.¹ The absorption characteristics of the film are affected by both the number and the states occupied by the photoexcited electrons. Similarly, the number and occupation of hole states generated by photon absorption will have an impact on the absorption of the film. Conduction electrons with $E_D > 0$ (*hot electrons*), lose energy primarily through electron-phonon (e-p) collisions. The initial excitation and subsequent relaxation of the electron and hole distributions induce changes in the absorption spectrum.¹ Measurement of

the changes in absorption during hot electron relaxation is an important goal of this study and should help lay the foundation for improved thermal engineering in photonic devices.

CARRIER THERMALIZATION AND RELAXATION PROCESSES

In direct gap semiconductors, photon absorption above the fundamental absorption edge occurs primarily by interband transitions, resulting in electron-hole pair generation. Following this, the electron system is left in an excited state and will return to a lower energy state through various relaxation processes. The hole system follows a similar process, but the discussion here will be limited to the electron system. In this discussion it will also be necessary to consider absorption occurring on extremely short time scales. The experiments presented here use laser pulses ~ 135 fs in duration, but even shorter pulses are possible. Absorption on this time scale produces a coherent redistribution of the electron system representative of the participating transitions. In the case of excitation by monochromatic light, initially the hot electron distribution will be sharply peaked in the region of the direct transition for that energy. Through thermalization and relaxation processes, the hot electrons will scatter to the bottom of the conduction band before recombining.⁵

These processes occur on time scales ranging from ~ 200 fs to greater than 100 ps, thus it is useful to consider several regimes of interest.¹ Table 1 lists these and the respective relaxation and scattering processes occurring in each.¹ These regimes are useful for characterizing the hot carrier distribution. Initially in the *Coherent Regime*, it is possible to have a discontinuous hot carrier distribution. Thermalization of the hot carriers will occur during this period through scattering processes in order to reach a continuous, yet nonthermal distribution. In the following *Nonthermal Regime*, relaxation through collisions begins to occur as hot carriers drop towards the conduction band minimum, releasing energy through collisions with optical phonons. Further relaxation occurs

in the *Hot Excitation Regime* through additional collisions with acoustic phonons. These leave the electrons near the conduction band minimum in the *Isothermal Regime* when recombination occurs.

The scattering rates of these processes vary depending on the carrier concentration as well as the film temperature. The density of photoexcited carriers will have a strong effect on electron-electron ($e-e$) scattering as well as screening effect on the $e-p$ scattering.¹ Experiments to observe $e-e$ scattering in GaAs films have been pursued by other groups at low temperatures.^{5,6} Under these conditions, this process will dominate in samples of high purity, but at room temperature and low carrier densities, the $e-e$ scattering rate (τ_{ee}^{-1}) is significantly less than the electron-phonon ($e-p$) scattering rate (τ_{ep}^{-1}).⁷ At sufficiently high carrier densities, $e-e$ scattering may become important, and will be examined as part of this study.

EFFECT ON OPTICAL PROPERTIES

Considering an ultrashort laser pulse with photon energy, E_g , greater than the band gap, E_g , absorption will occur primarily through interband transitions resulting in the generation of hot electrons. This will result in a reduction in the number of states available for photon absorption. Initially, absorption near the excitation energy is suppressed, but as the hot electrons relax, the absorption will increase. As the hot carrier distribution changes due to the various scattering processes, the absorption characteristics of the film change as well. Transient changes in the hot carrier distribution cause a transient change in the observed reflectance of the film, DR/R .

The reflectance for near normal incidence is commonly expressed as a function of the complex index of refraction $n = n_1 + in_2$,

$$R = \frac{(n_1 - 1)^2 + n_2^2}{(n_1 + 1)^2 + n_2^2} \quad (1)$$

or in terms of the dielectric constant, ϵ , where

$$n_1 + in_2 = \sqrt{\mathbf{e}} = \sqrt{1 + 4\mathbf{p}\mathbf{c}}. \quad (2)$$

To understand how the dynamics of the hot carrier distribution affect the reflectance, it is necessary to examine the interband model for the electric susceptibility⁸,

$$\mathbf{c}_v = \frac{e^2}{4\mathbf{p}^2 m} \int \frac{f_{jvk}(\mathbf{w}_{jvk})}{\mathbf{w}_{jvk}^2 - \mathbf{w}^2} \mathbf{h}_v(\mathbf{w}_{jvk}) d\mathbf{w}_{jvk}. \quad (3)$$

Here, jvk denotes the transition of an electron from band v j with crystal momentum k , $f_{jvk}(\mathbf{w}_{jvk})$ is the oscillator strength of the transition, and $\mathbf{h}_v(\mathbf{w}_{jvk})$ is the density of states in the interval from \mathbf{w}_{jvk} to $\mathbf{w}_{jvk} + d\mathbf{w}_{jvk}$. In this model, the photoexcited carriers would be represented as a decrease in the density of states at transitions linking states newly occupied by electrons in the conduction band, or holes in the valence band. As the carriers scatter and relax, the states available for transitions will change. The resulting change in \mathbf{c}_v produces a change in R . The modulation technique used in these experiments allows for detection of very small changes in R .

It is important to note that significant changes in the reflectance can occur as the photon energy is increased above the threshold for certain transitions. Examination of the band structure of InP reveals transitions from the spin-orbit split-off (s-o) band to the conduction band with energy above $E_g + \mathbf{D}$, in addition to the direct transitions originating from the top of the valence band (E_g). Transitions from the s-o band are allowed through part of the tuning range of the laser. In doped crystals, the donor and acceptor states can also participate in the absorption processes⁹ as well as cause band narrowing at high concentrations^{10,11}. These transitions must be taken into account in the calculation of \mathbf{c}_v when necessary.

EXPERIMENTAL SETUP

The experimental setup used for this study is depicted in Fig. 1. A passively mode-locked Ti:Sapphire laser is used to produce the ultrashort pulses ($t_p \sim 135$ fs) required for this study. The pulses are generated at a repetition rate of 76 MHz and are tunable over a wavelength range of 720 - 860 nm. The beam is split and follows two paths, the pump and the probe path. In the probe

beam path, a half-wave plate rotates the polarization by 90° to allow scattered pump light to be eliminated by a polarizer before detection. The pump and probe beams are focused onto the sample with a diameter of $\sim 35 \mu\text{m}$ and $\sim 5 \mu\text{m}$ respectively. The probe is focused at the center of the pump beam on the sample, ensuring isometric excitation in the plane of the film at the probe beam focus. The pump path length is fixed while the probe path length can be varied using a linear micropositioning stage. This allows for control of the probe path length in less than 10 fs increments such that the probe pulse arrives before, during, or after the pump pulse. The pump beam is modulated by an acousto-optic modulator (AOM) at 1 MHz resulting in a modulated excitation of the sample, enabling small signal detection with a lock-in amplifier. The modulated carrier distribution produced by the pump beam causes a modulation of the optical properties. The initial excitation and subsequent relaxation of the hot carrier distribution are detected through transient reflectance data.^{1,12} Data scans are taken by recording the magnitude and phase of the 1 MHz photodetector response as the probe path is varied in discrete steps. Phase information in the detected signal can be used in post processing of the data to subtract any nontransient noise.¹³ The dc voltage of the photodetector is recorded for each scan and used to scale the signal measured by the lock-in.

In an effort to further isolate the reflected probe light, measurements were made to detect any photoluminescence (PL) resulting from the laser excitation. This was achieved by passing all possible collected light from the sample through a monochromator and onto the photodetector. No measurable PL signal could be detected and it is not expected to contribute significantly to the signal seen by the detector.

RESULTS

The measurements presented in this paper were performed using ultrashort laser pulses with a pulse width of $t_p \sim 135$ fs, thus the *Nonthermal* and *Hot-Excitation Regimes* will be the timescales

of primary interest. Since no measurable PL signal is detected, recombination during the *Isothermal Regime* is not observed. It is also not clear whether processes occurring in the *Coherent Regime* can be detected due to the time scales of interest relative to t_p . The goal of this investigation is to explore and identify relevant characteristics of femtosecond transient reflectance data taken on materials used for photonic devices. In particular, *DR/R* scans have shown a significant dependence on the photon energy of the excitation as well as some dependence on the pump fluence.

The experiments presented here were performed on an intrinsic, a Se doped n-type, and a Zn doped p-type InP film. The specifications for each sample are shown in Table 2. For each film, scans were taken at several pump intensities over a range of photon energy from 1.443 eV to 1.723 eV, well above the measured band gap for these films ($E_g = 1.32$ eV). This interband model is a good representation of absorption in this region and attention must be paid to transitions that become available above certain energies. All of the *DR/R* scans cover 1500 ps of delay and exhibit many similar features. In each, the initial excitation of the probe is seen as a sharp increase in the reflectance, or *DR/R* signal. This signal then decays towards zero, but the shape of this decay varies both with photon energy, E_g , and pump intensity. The peak of the *DR/R* signal is on the order of 10^{-3} for all of the samples at all energies. To help illustrate the features of interest in these scans, it is useful to normalize the scans.

In Fig. 2, normalized *DR/R* scans of the intrinsic InP film are shown for a 100 mW pump power. The photon energy is labeled for each scan, and an inset plot of the first 6 ps is shown with the highest and lowest energy highlighted. In general, the higher energy scans exhibit a faster decay in the *DR/R* signal, but the transition occurs abruptly as E_g is increased from 1.477 eV to 1.591 eV. This indicates faster scattering rates out of the initial excitation states at higher energies. By examining the scans within the first few picoseconds another feature is seen to develop as a function of the photon energy. A dramatic change in the initial response to the pump excitation appears only

at the lowest energy, 1.443 eV. In this scan, a faster initial rise followed by a decrease precedes the slower response that quickly dominates the signal.

In Fig. 3, scans of the n-type sample are plotted and exhibit many of the same features seen in the intrinsic sample. The change in the decay of the DR/R signal is again seen to occur between 1.513 eV and 1.591 eV. Also, the initial fast transient appears in the lowest energy scan, but is less pronounced. Scans of the p-type sample depicted in Fig 4 once again indicate a change in the decay of the DR/R signal across the same spectral region. It is not clear at this point whether this is attributed to any physical processes or a malfunction in the experiment. The 1.443 eV scan has the same fast transient feature as in the other samples.

The change in the decay of the DR/R signal seems to coincide with the energy required for the transition from the split-off band to the conduction band. The s-o band has been reported to lie $\sim 0.11 \sim 0.20$ eV below the primary valence band maximum at G_{15} .^{4,14} This results in a transition energy of $\sim 1.43 \sim 1.52$ eV, which is close to the energy at which the decay in the scans begins to change. It is not clear at this point how these additional states affect the scattering processes involved in the relaxation of hot carriers, but it does appear to contribute in a similar way for every sample. The fast transient appearing in the 1.443 eV scans may also be related to the s-o band transition. If the transition lies just below this photon energy, even small perturbations to the band structure could cause significant changes to the number of states available for a transition. Such a perturbation could arise from an effect such as band gap narrowing due to a high carrier concentration as reported by Bugajski and Lewandowski.¹¹ Considering the significant kink in the absorption spectrum at the s-o band energy¹⁵, a strong response in the DR/R signal could be expected in this region of the spectrum.

In addition to varying E_g , the pump intensity was also varied to examine the effect of the carrier concentration on the DR/R response. Scans were taken at 50 mW, 100 mW, and 200 mW at each E_g

except 1.723 eV where the power of the pump beam was limited to less than 200 mW. An additional scan was taken at each E_g at the highest intensity possible. The results were similar over the range of E_g , and a plot of the intrinsic sample at 1.551 eV is shown in Fig. 5. It appears that the decay of the DR/R response is faster at lower carrier densities (i.e. lower pump intensity). The cause of this effect has not been determined but could be the result of the relatively long lifetime of the carriers compared to the relaxation rates. The excess carriers in the conduction band effectively reduce the number of transitions available for absorption. In this case, e-h recombination could be observed indirectly as a function of the relative number of available states.

CONCLUSIONS

Experiments presented here for several InP based films have demonstrated the sensitivity of the transient reflectance signal to both photon energy and the number of excited carriers. Experimental DR/R scans seem to indicate a change in the transient behavior of the films above the energy required for transitions originating from the spin-orbit split-off band. To form a more complete understanding of the DR/R signal, the actual values of the n_1 and n_2 must be measured across the spectral range of the laser for each sample. This will enable a more accurate calculation of the excited carrier density generated by the pump pulses and aid in developing an accurate transient reflectance model. In this study, the pump and probe photon energy are equal, so the probe effectively monitors the rate at which electrons (and holes) are scattered out of the initial excited states. Future studies have been proposed to enable probing states below the excited states in order to further resolve the nature of the scattering processes involved.

ACKNOWLEDGEMENTS

The authors would like to thank the National Science Foundation (CTS-9908372) and the Virginia Space Grant Consortium for their support of this work.

REFERENCES

- ¹Jagdeep Shah, in *Hot Carriers in Semiconductor Nanostructures - Physics and Applications*, edited by Jagdeep Shah (Academic Press, 1992).
- ²S. W. Koch, F. Jahnke, and W. W. Chow, *Semiconductor Science Technology* **10**, 739 (1995).
- ³H. Barry Bebb and E. W. Williams, in *Transport and Optical Phenomena*, edited by R.K. Willardson and Albert C. Beer (Academic Press, 1972), Vol. 8.
- ⁴V. Swaminathan and A.T. Macrander, *Materials Aspects of GaAs and InP Based Structures*. (Prentice Hall, 1991).
- ⁵Jagdeep Shah, *Solid-State Electronics* **21**, 43 (1978).
- ⁶W. Z. Lin, L. G. Fujimoto, and E. P. Ippen, *Applied Physics Letters* **50** (3), 124 (1987).
- ⁷Charles Kittel, *Introduction to Solid State Physics*, 7th ed. (Wiley, New York, 1996).
- ⁸W. G. Spitzer and H. Y. Fan, *Physical Review* **106** (5), 882 (1957).
- ⁹J. U. Fischbach, G. Benz, N. Stath, and M. H. Pilkuhn, *Solid State Communications* **11**, 725 (1972).
- ¹⁰S. C. Jain, J. M. McGregor, and D. J. Roulston, *Journal of Applied Physics* **68** (7), 3747 (1990).
- ¹¹M. Bugajski and W. Lewandowski, *Journal of Applied Physics* **57** (2), 521 (1985).
- ¹²H. Y. Fan, in *Optical Properties of III-V Compounds*, edited by R. K. Willardson and Albert C. Beer (Academic Press, 1967), Vol. 3.
- ¹³Andrew N. Smith, Andrew P. Caffrey, J. Michael Klopff, and Pamela M. Norris, presented at the 35th National Heat Transfer Conference, Anaheim, CA, 2001.
- ¹⁴Marvin L. Cohen and James R. Chelikowsky, *Electronic Structure and Properties of Semiconductors*. (Springer-Verlag, New York, 1989).
- ¹⁵Manuel Cardona, in *Optical Properties of III-V Compounds*, edited by R. K. Willardson and Albert C. Beer (New York, 1967), Vol. 3.

Table 1: Transient Thermalization and Relaxation Regimes¹

<u>TIME SCALES FOR THERMALIZATION AND RELAXATION OF HOT CARRIERS</u>	
	<p><i>Coherent Regime</i> (≈ 200 fs)</p> <ul style="list-style-type: none"> • momentum scattering • carrier-carrier scattering • intervalley scattering ($G \rightarrow L, X$) • hole-optical phonon scattering
	<p><i>Nonthermal Regime</i> (≈ 2 ps)</p> <ul style="list-style-type: none"> • electron-hole scattering • electron-optical phonon scattering • intervalley scattering ($L, X \rightarrow G$) • intersubband scattering ($\Delta E > \hbar \omega_{LO}$)
	<p><i>Hot Excitation Regime</i> ($\sim 1 \sim 100$ ps)</p> <ul style="list-style-type: none"> • hot carrier-phonon interactions • decay of optical phonons • carrier-acoustic phonon scattering • intersubband scattering ($\Delta E < \hbar \omega_{LO}$)
	<p><i>Isothermal Regime</i> (≈ 100 ps)</p> <ul style="list-style-type: none"> • carrier recombination
<i>Time</i>	

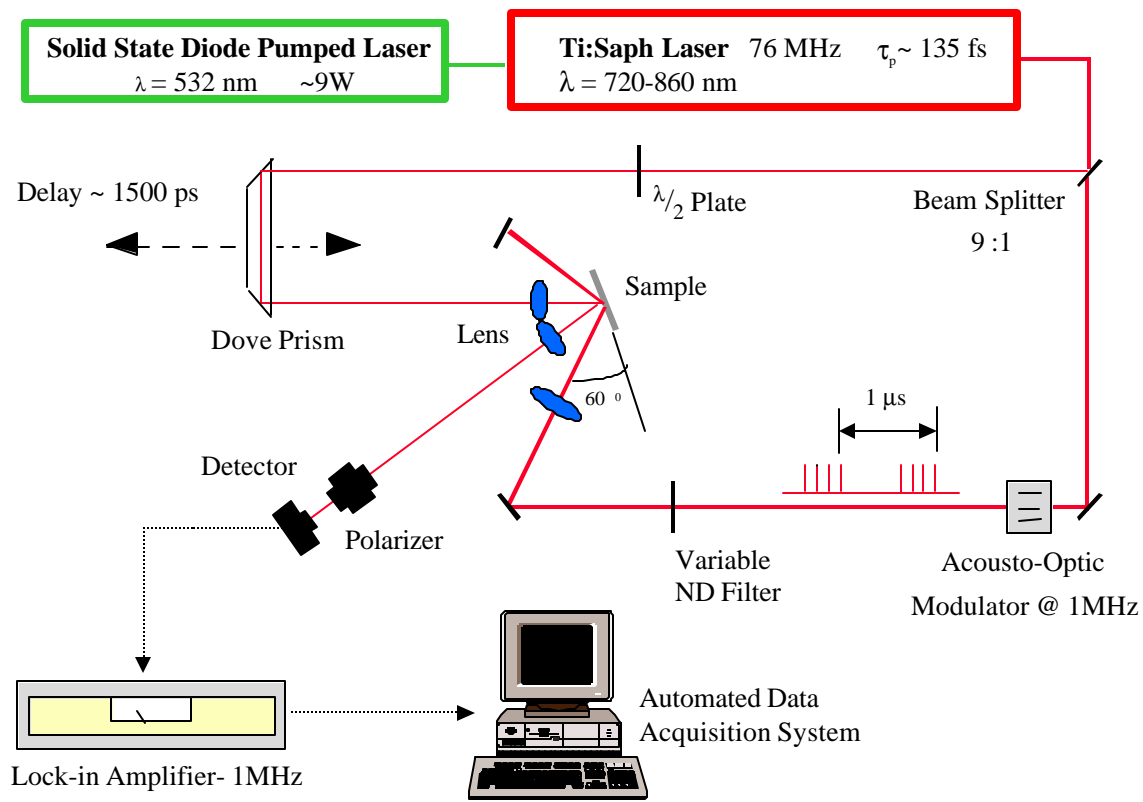


Figure 1: Experimental setup for spectrally resolved transient reflectance measurements.

Table 2: Composition and Thickness of Each Sample

	<i>InP</i>	<i>InP n-type</i>	<i>InP p-type</i>
film material	InP	InP:Se	InP:Zn
thickness	2142 nm	1020 nm	1020 nm
doping	-	$n = 1.7 \times 10^{18} \text{ cm}^{-3}$	$p = 1.2 \times 10^{18} \text{ cm}^{-3}$
E_g	1.32 eV	1.32 eV	1.32 eV
substrate	InP:S	InP:Fe	InP:S

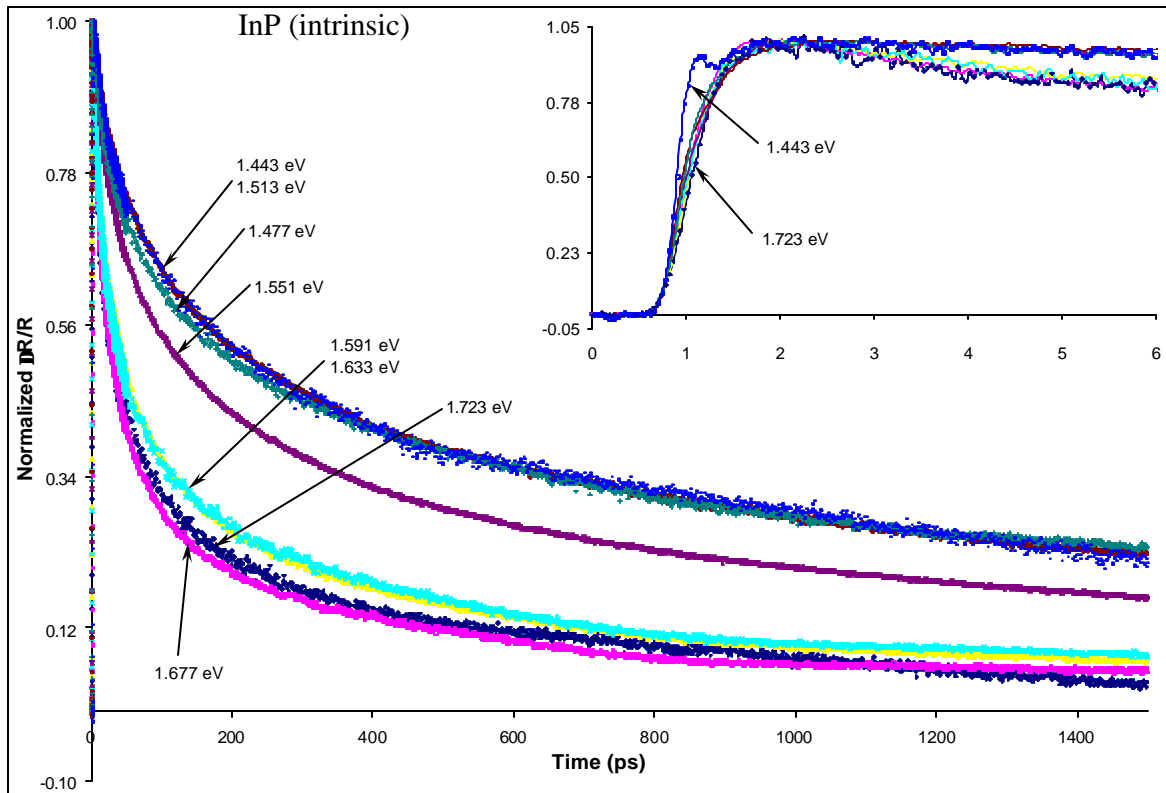


Figure 2: Normalized DR/R scans for the InP (intrinsic) film with a 100 mW pump beam. Scans are labeled according to the photon energy. The inset plot shows the first 6ps of each scan, with the highest and lowest energy scans highlighted.

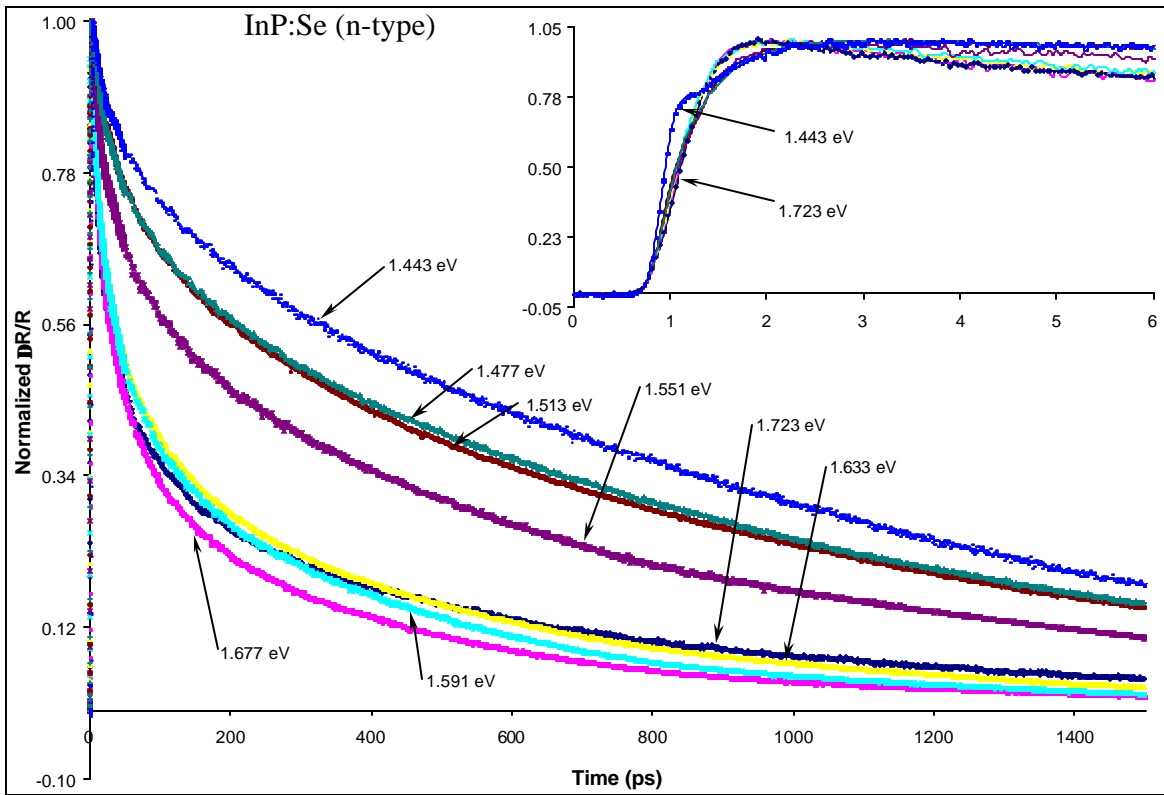


Figure 3: Normalized DR/R scans for the InP:Se (n-type) film with a 100 mW pump beam.

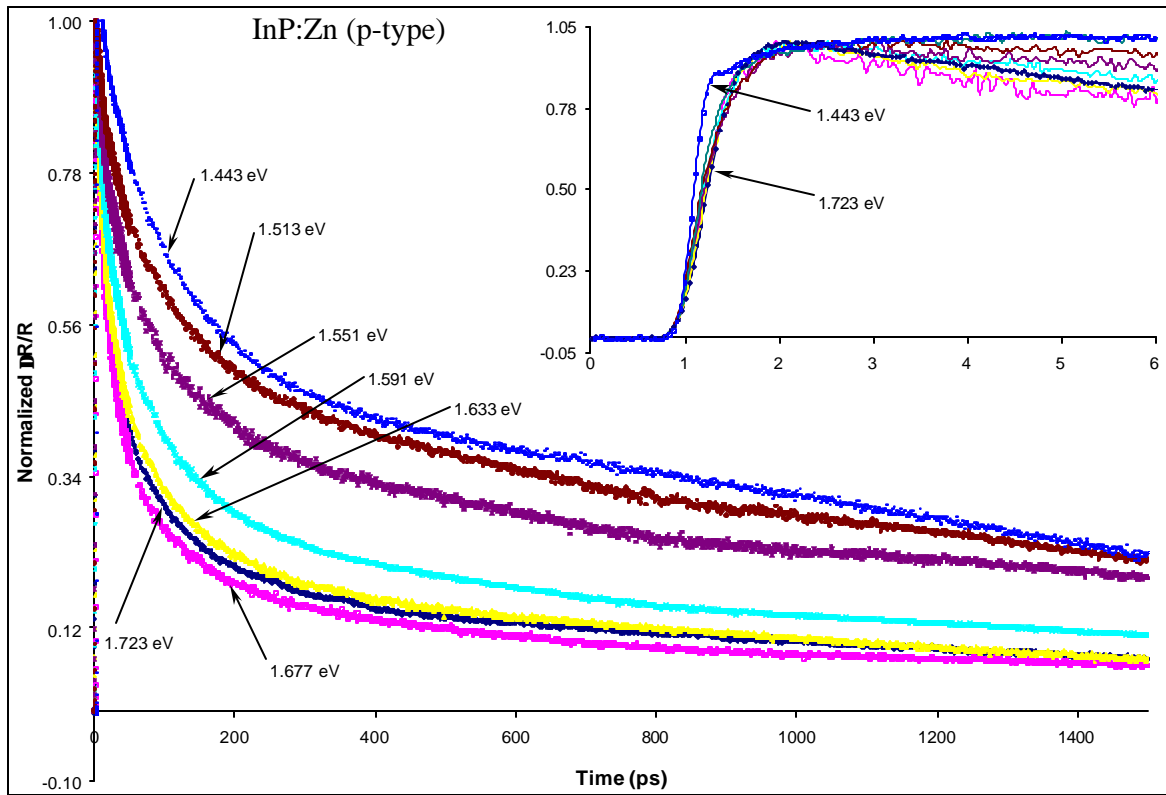


Figure 4: Normalized DR/R scans for the InP:Zn (p-type) film with a 100 mW pump beam.

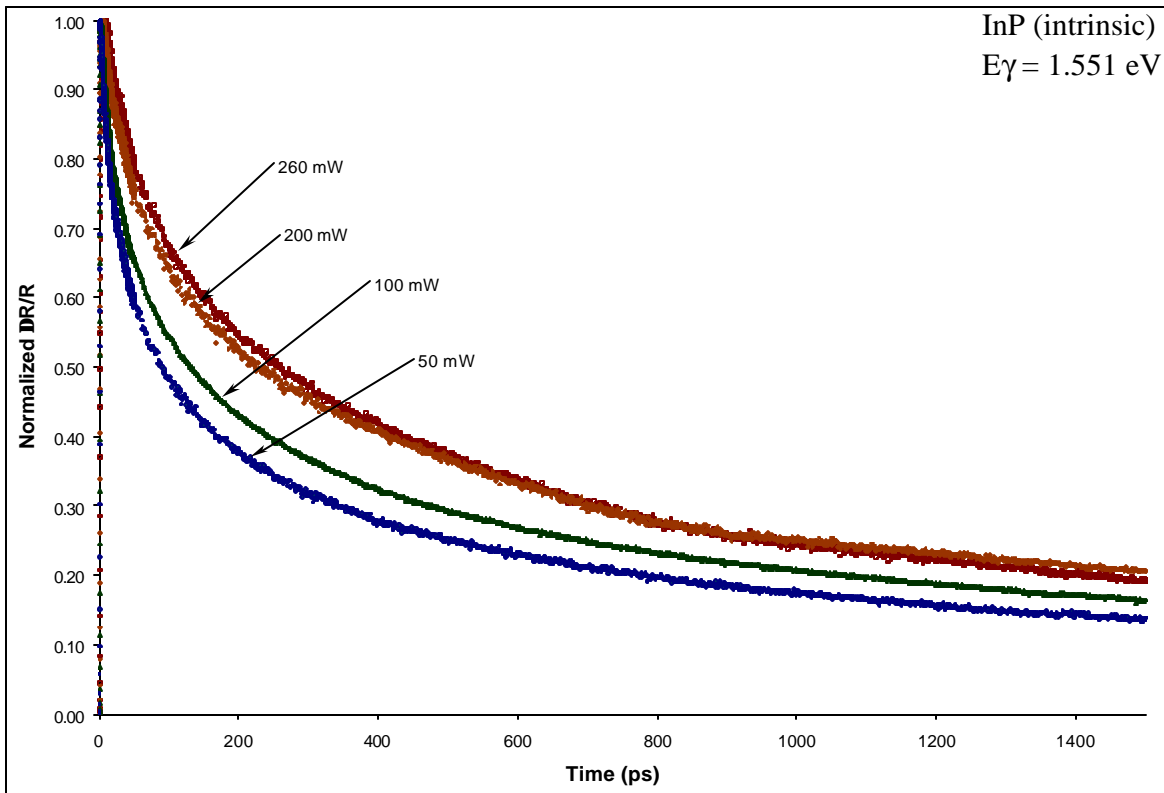


Figure 5: DR/R scans for the InP (intrinsic) film at varying pump intensities.